RESEARCH ARTICLE

Evidence of Protein Binding by a Nucleopeptide Based on a Thymine-decorated L-Diaminopropanoic Acid through CD and *In Silico* Studies

Valentina Roviello[1,#], Domenica Musumeci[2,3,#], Andriy Mokhir[4] and Giovanni N. Roviello[3,*]

[1]*Department of Chemical, Materials and Industrial Production Engineering (DICMaPI), University of Naples Federico II, Piazzale V. Tecchio 80, 80125 Naples, Italy;* [2]*Department of Chemical Sciences, University of Naples Federico II, Via Cintia 21, 80126 Naples, Italy;* [3]*Institute of Biostructures and Bioimaging (IBB) - CNR, Via Mezzocannone 16, 80134 Naples, Italy;* [4]*Department of Chemistry and Pharmacy, Friedrich Alexander University, Nikolaus-Fiebiger-Str. 10, 91058 Erlangen, Germany*

Abstract: ***Background***: Nucleopeptides are chimeric compounds of biomedical importance carrying DNA nucleobases anchored to peptide backbones with the ascertained capacity to bind nucleic acids. However, their ability to interact with proteins involved in pathologies of social relevance is a feature that still requires investigation. The worrying situation currently observed worldwide for the COVID-19 pandemic urgently requires the research on novel anti-SARS-CoV-2 molecular weapons, whose discovery can be aided by *in silico* predictive studies.

Objective: The aim of this work is to explore by spectroscopic methods novel features of a thymine-bearing nucleopeptide based on L-diaminopropanoic acid, including conformational aspects as well as its ability to bind proteins, starting from bovine serum albumin (BSA) as a model protein. Moreover, in consideration of the importance of targeting viral proteins in the current fight against COVID-19, we evaluated *in silico* the interaction of the nucleopeptide with some of the most relevant coronavirus protein targets.

Methods: First, we investigated *via* circular dichroism (CD) the conformational behaviour of this thymine-bearing nucleopeptide with temperature: we observed CD spectral changes, particularly passing from 15 to 35 °C. Scanning Electron Microscopy (SEM) analysis of the nucleopeptide was also conducted on nucleopeptide solid samples. Additionally, CD binding and preliminary *in silico* investigations were performed with BSA as a model protein. Moreover, molecular dockings were run using as targets some of the main SARS-CoV-2 proteins.

Results: The temperature-dependent CD behaviour reflected the three-dimensional rearrangement of the nucleopeptide at different temperatures, with higher exposure to the solvent of its chromophores at higher temperatures compared to a more stacked structure at a low temperature. SEM analysis of nucleopeptide samples in the solid-state showed a granular morphology, with a low roughness and some thread structures. Moreover, we found through spectroscopic studies that the modified peptide bound the albumin target by inducing significant changes to the protein secondary structure.

Conclusion: CD and preliminary *in silico* studies suggested that the nucleopeptide bound the BSA protein with high affinity according to different binding modes, as testified by binding energy scores lower than -11 kcal/mol. Interestingly, a predictive study performed on 3CL[pro] and other SARS-CoV-2 protein targets suggested the potential ability of the nucleopeptide to bind with good affinity the main protease of the virus and other relevant targets, including the RNA-dependent RNA polymerase, especially when complexed with RNA, the papain-like protease, and the coronavirus helicase at the nucleic acid binding site.

*Address correspondence to this author at the Institute of Biostructures and Bioimaging (IBB) - CNR, Via Mezzocannone 16, 80134 Naples, Italy; Tel: +39 081 2534585; Fax: +39 081 2203498; E-mails: giroviel@unina.it, giovanni.roviello@cnr.it
[#] These authors contributed equally to this work.*

1. INTRODUCTION

Nucleopeptides are both synthetic and natural molecules composed of nucleobases inserted on a peptide backbone. Among the DNA analogues, nucleopeptides constitute a family of chimeric compounds with interesting features deriving from their experimentally ascertained ability to bind complementary DNA and RNA sequences permeating cellular membranes [1-6], as well as from their capacity to form supramolecular networks [7]. In this regard, structures containing single nucleobases are also interesting, such as synthetic nucleoside analogues [8-13], nucleoamino acids [14, 15] and peptidyl nucleosides [16-18], some of which were shown to act as building blocks for supramolecular networks of potential biomedical relevance [19-22]. Additionally, the incorporation of single nucleobase-bearing amino acid units into polyamino acid chains can stabilize peptide and protein structures, leading to enhancement of their function [23, 24]. Moreover, *in sero*-stable mononucleobase-bearing dipeptides were able to interact with serum albumins [19], whilst a single thymine-functionalized peptide bound the reverse transcriptase (RT) of Human Immunodeficiency Virus (HIV), inhibiting its activity [25]. However, the ability of nucleopeptides to interact with proteins has not yet been explored in detail, with only a few examples reported in the literature such as evidence of binding to the Moloney murine leukemia virus (MMLV) RT by nucleobase-bearing peptides [26].

Here, we investigated the ability of a nucleopeptide based on L-diaminopropanoic acid (here below simply indicated as nucleopeptide), previously described by us as a DNA and RNA binder [27], to interact with proteins, using bovine serum albumin (BSA) as a model system. We used circular dichroism (CD) spectroscopy to show changes in the secondary structure of proteins and peptides caused by ligand binding [28]. To give more detailed information on the nature of the resulting complex, we also performed *in silico* studies. In fact, *in silico* molecular docking has recently emerged as a fundamental tool to predict the precise docking site of ligands onto protein/peptide complexes and other relevant properties. Among the many applications of *in silico* modelling, several recent literature examples report on its utility in determining the structure of molecular scaffolds, their plasmonic properties, and functional aspects such as antibacterial properties [29-31]

Finally, a preliminary docking study was also performed on the interaction of the nucleopeptide with several proteins essential for SARS-CoV-2, the virus at the origin of the current pandemic COVID-19 [32-34]. The COVID-19-related targets in our investigation included the main protease 3CL^{pro}, the papain-like protease [35, 36], the coronavirus helicase [37] and the RNA-dependent RNA polymerase (RdRp) [38]. The molecular modelling analysis on the RdRp target was performed in the absence or presence of RNA, taking into consideration the intrinsic ability of the nucleopeptide to bind RNA molecules.

2. EXPERIMENTAL SECTION

2.1. Chemicals

The nucleopeptide (hexathymine dodecadiaminopropanoic acid) was obtained by solid-phase peptide synthesis [39, 40], as previously described by us [27]. All solvents, buffers and chemicals were purchased by Sigma Aldrich. PBS (phosphate buffer saline) was as follows: 137 mM NaCl, 2.7 mM KCl, 10 mM Na_2HPO_4, 1.8 mM KH_2PO_4.

2.2. CD Experiments

CD spectra were obtained on a Jasco J-715 spectropolarimeter coupled to a PTC-348WI temperature control system, using Hellma quartz cells with path length of 2 x 0.4375 cm (tandem cell) or 1 cm, and the following parameters: response of 1 s, scanning speed of 100 nm/min and bandwidth of 2.0 nm. All the spectra were averaged over three scans.

The temperature-dependent CD study on unbound nucleopeptide (8 μM in 10 mM phosphate buffer, pH 7.5) was performed in the 15-95 °C temperature range using the 1-cm cell (3 mL overall volume).

The CD-binding experiment was conducted, analogously to previous works [2, 14, 26, 41-49], in the tandem cell, using a 0.1 μM concentration of BSA in PBS (2 mL overall volume, pH 7.5) and 6.4 nmol of nucleopeptide ligand, at 5 °C.

Secondary structure percentages of BSA, free and complexed to the nucleopeptide, were determined by Bestsel [50] (http://bestsel.elte.hu/) and K2D2 [51] (http://cbdm-01.zdv.uni-mainz.de/~andrade/k2d2/) deconvolution programs using the spectra obtained in the CD-binding experiment.

2.3. Scanning Electron Microscopy (SEM) Analysis

Samples for microscopic observations were obtained using the compound in solution. After slow solvent evaporation, the sample containing the nucleopeptide was coated with a conductive layer of Au-Pd and examined in a Nova NanoSem 450 FEI SEM at 2.00
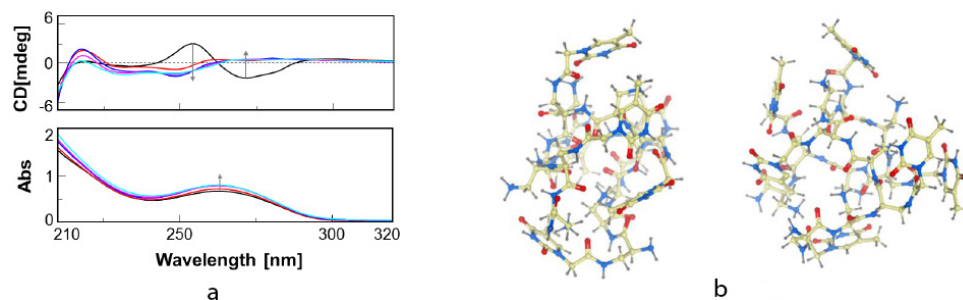
Fig. (1). a. Overlapped CD spectra of an 8 μM nucleopeptide solution in 10 mM phosphate buffer, pH 7.5, at 15 (black), 35 (red), 55 (blue), 75 (magenta), and 95 (cyan) °C; **b**. 3D structure representation of the nucleopeptide as obtained by energy minimization with ICM 2D to 3D software (https://www.molsoft.com/2dto3d.html). (*A higher resolution / colour version of this figure is available in the electronic copy of the article*).

and 3.00 kV in high vacuum mode, in analogy to previous works [44, 52-54].

2.4. SwissDock Protein Docking Experiments

Target protein structures were obtained from the Protein Data Bank (PDB) [55]. Positively charged ligand structure edited in 'ChemDraw and suitably prepared was converted to MOL2 file with Pasilla converter (http://pasilla.health.unm.edu/tomcat/biocomp/convert) and used for the subsequent studies. Dockings of the nucleopeptide to BSA (PDB: ID 4f5S, chain A) and to unliganded 3CL^{pro} (PDB: ID 6y84) were performed by SwissDock, server based on the docking software EA-Dock DSS [56]. Docking experiments were obtained after 250 consecutive runs. The most energetically favourable binding modes, evaluated by the Fast Analytical Continuum Treatment of Solvation (FACTS) method [57], were clustered. Clusters were then ranked according to the full fitness scores. Docking results were visualized in the UCSF Chimera package [58].

2.5. Multiple COVID-19 Protein Docking Experiments

Computational studies on the possible interaction of the nucleopeptide with different SARS-CoV-2 protein targets were achieved by the COVID-19 Docking Server, a user-friendly platform realized by Kong et al. for docking small molecules, peptides and antibodies against COVID-19-related targets by implement of Autodock Vina and CoDockPP as docking engines [59-63]. We selected in the COVID-19 Docking Server (for ligand preparation, PDB IDs and description of protein targets, scoring and docking procedures see https://ncov.schanglab.org.cn/) as 'Computational

Type': 1-molecule Docking, and as coronavirus protein targets the following: 'Main protease; Papain-like protease; Nsp3 (207-379, AMP-binding site); Nsp3 (207-379, MES-binding site); RdRp (RTP-binding site); RdRp (RNA-binding site); Helicase (ADP-binding site); Helicase (NCB site); Nsp14 (ExoN); Nsp14 (N7-MTase); Nsp15 (endoribonuclease); Nsp16 (G-TA-binding site); Nsp16 (MGP-binding site); Nsp16 (SAM-binding site); N protein (NCB-binding site)'. After multiple docking runs, the server provided the pose views for the different binding modes, and the corresponding binding energy (score value, kcal/mol) and scoring function (RF-Score, pKd) values. RdRp-nucleopeptide complexes in the presence or absence of RNA were visualized in the COVID-19 Docking Server (https://ncov.schanglab.org.cn/). Listed values of score values and RF score values for the top 10 poses for RdRp/nucleopeptide and RdRp+RNA/nucleopeptide in Table **S6** were obtained as the output of the docking experiments performed by the COVID-19 Docking Server.

3. RESULTS AND DISCUSSION

3.1. Investigation of Nucleopeptide Conformation at Different Temperatures

First, we studied the spectroscopic behaviour of the nucleopeptide in the aqueous buffer by CD, heating the solution up to 95°C and recording CD spectra at regular temperature intervals (Fig. **1A**).

A dramatic change of the CD profile passing from 15 to 35 °C was revealed. In particular, both the positive band at 254 nm and the negative one at 273 nm, observed in the spectrum at 15 °C (black line), disappeared (Fig. **1A**, up). This suggested that the nucleopeptide was able to adopt different conformations at
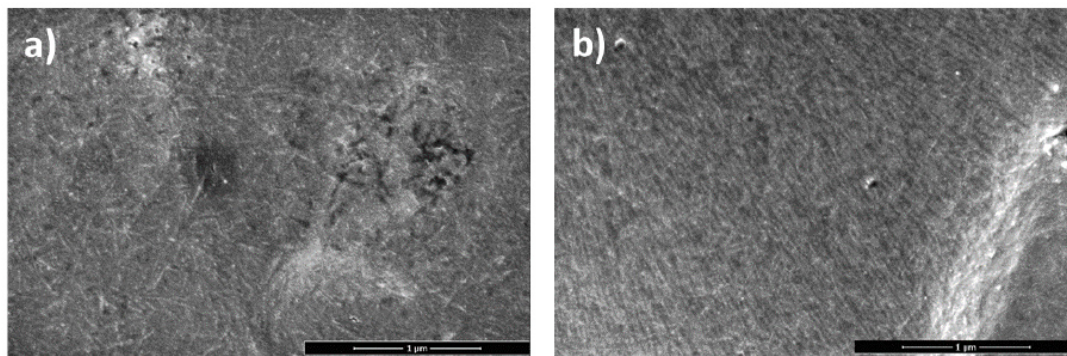
Fig. (2). SEM micrographs of the nucleopeptide at 100000x, 1μm. (*A higher resolution/colour version of this figure is available in the electronic copy of the article*).

different temperatures with a higher degree of structuration at lower temperatures. UV-absorbance monitoring upon increasing the temperature (Fig. **1A**, bottom) also confirmed the CD behaviour: a hyperchromic effect of the aromatic band at 264 nm was, in fact, observed going from 15 to 35 °C, suggesting a more stacked situation at lower temperatures, with a substantial stabilization at 55 °C.

To obtain a picture of the three-dimensional structure of the nucleopeptide and tentatively to explain the stacked conformation of the molecule at the low temperature suggested by the CD and UV thermal trend, we performed *in silico* 3D structure prediction using ICM 2D to 3D converter (Molsoft, LLC) obtaining the energy-minimized structure reported in Fig. (**1B**). It was evident that the nucleopeptide at its lowest energy state tended to adopt a conformation in which it was at least partially compact. This could explain the lower UV absorbance at low temperatures because of the spatial proximity of stacking thymine rings, evidently lost during the heating process.

3.2. SEM Analysis

The morphology of a nucleopeptide sample was also investigated in the solid phase by SEM. Imaging of dried nucleopeptide (droplet from a 400 μM solution in H_2O) led to the SEM micrographs shown in (Fig. **2**).

The surface morphology of the sample appears granular, with low roughness and some thread structures (Fig. **2a**). In fact, several dense and long thread structures of ~20 nm thickness were clearly detected (Fig. **2b**). Interestingly, this morphology is similar to those already described in the literature for other peptide/nucleopeptide derivatives observed by SEM microscopy [64].

3.3. Nucleopeptide-protein CD Binding Studies

With the aim of exploring the ability of the nucleopeptide to interact with proteins, we performed a CD experiment by using a tandem cell. First, we recorded the CD spectrum of BSA and nucleopeptide, contained as separated solutions in the two compartments of the cell, as a single sum spectrum: it resulted in a spectrum almost identical to that of the protein alone (Fig. **3**, black line) since the nucleopeptide did not show a significant contribution to the CD signal at the concentration used. Then, after mixing of the solutions obtained by manual rotation of the quartz cell, the resulting spectrum (Fig. **3**, red line) showed some differences with respect to the sum spectrum: *i.e.* the CD profile of the protein changed after ligand mixing.
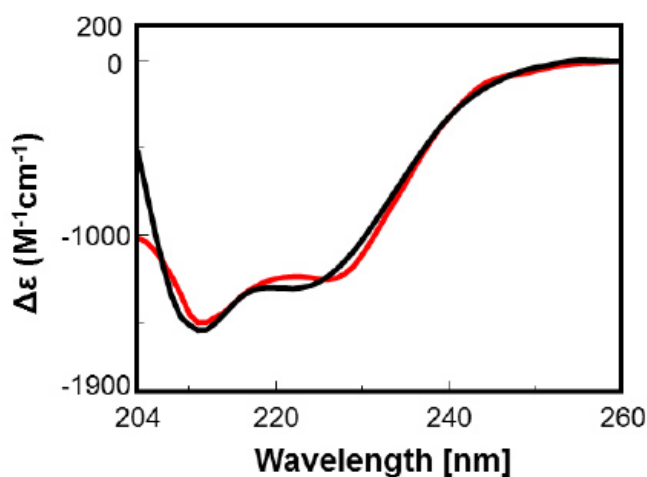

Fig. (3). Overlapped CD spectra of BSA (0.1 μM) - nucleopeptide (3.2 μM) in PBS recorded as separated (sum spectrum, **black line**) or mixed solutions (**red**) in the tandem cell. (*A higher resolution/colour version of this figure is available in the electronic copy of the article*).

In this way, we demonstrated that the nucleopeptide was able to bind a protein, in particular the BSA, inducing variation of its secondary structure. Furthermore, by CD spectra deconvolution, realised by two deconvolution programs [50, 51] we could conclude that the nucleopeptide provoked a decrease in α-helix content higher than 10% and an increase in the β-sheet degree (Table **1**).

Table 1. Variations in α-helix and β-sheet secondary structure percentages for BSA and BSA/nucleopeptide complex as determined by deconvolution of CD spectra with Bestsel (A) and K2D2 (B) methods.

$\Delta(\%_{complex}-\%_{BSA})$		
-	**A**	**B**
α-helix	-14.0%	-11.0%
β-sheet	+14.1%	+4.2%

3.4. Molecular Docking

The interaction with BSA was also investigated by preliminary *in silico* studies. In fact, we docked the nucleopeptide ligand to the helix-rich [65] BSA structure (PDB: ID 4f5s [66]) and selected the poses with the best full fitness scores (Table **S1**). As shown in Fig. (**4**) (up), the nucleopeptide has two main docking clusters, all corresponding to energy scores lower than -11 kcal/mol (Table **S1**) and reflecting the binding to helical regions of the BSA chain A (Fig. **4**, up), as revealed by UCSF Chimera (data not shown), according to the CD evidence on alteration of the helical protein content upon ligand recognition Fig. (**3**) (Table **1**). Thus, this nucleopeptide, besides interacting with complementary DNA and RNA as we previously found [27], can also bind proteins forming complexes endowed with high affinity, as we showed here *in vitro* by CD experiments and *in silico* by docking studies (Figs. **4** and **S1**).

cluster 0 rank 0; -11.79   cluster 1 rank 0; -11.64

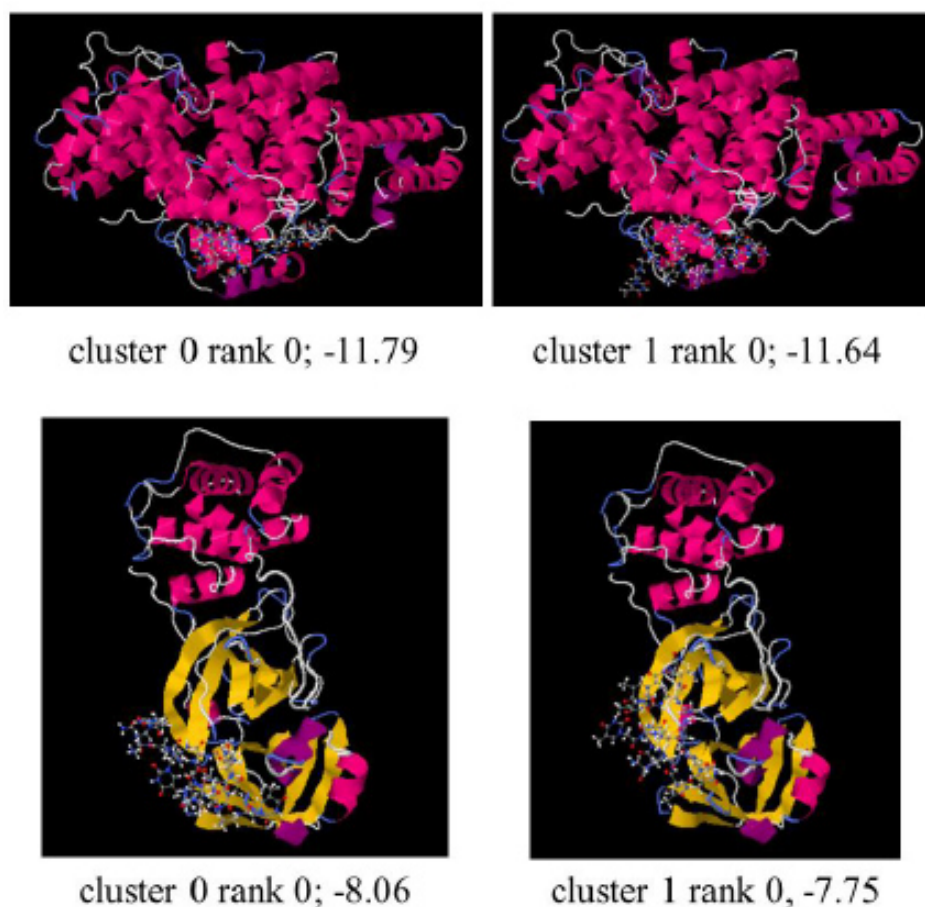cluster 0 rank 0; -8.06   cluster 1 rank 0, -7.75

Fig. (4). SwissDock pose views of clusters 0 and 1 (ranks n. 0, with binding energy scores in kcal/mol) for the predicted complexes formed between BSA (**up**) and 3CL^pro (**bottom**) with the nucleopeptide. (*A higher resolution / colour version of this figure is available in the electronic copy of the article*).

Since BSA was essentially a model protein and not a biomedical target, we also decided to study the potential for the nucleopeptide to target proteins of therapeutic importance, and with this aim, we docked it to the unliganded SARS-CoV-2 3CL^{pro} (PDB: ID 6y84 [67]). The results obtained by SwissDock software [68, 69] are shown in Table **S1**. For the top-ranked docked conformation (belonging to cluster 0) a full fitness score of -923.78 kcal/mol and a ΔG of -8.06 kcal/mol were estimated. Similar scores were found for the top-ranked pose from cluster 1 (Table **S2**). Both ΔG energy and full fitness scores were comparable to those previously reported in the literature for the conjugate noscapine-hydroxychloroquine (Nos-Hcq), based on which the authors predicted for Nos-Hcq a high M^{pro}-binding potential and effectiveness as therapeutic for SARS-CoV-2 [70]. As can be observed from Fig. (**4**. bottom), our prediction suggested that the nucleopeptide-3CL^{pro} interaction involved a β-sheet-rich region of the protease (domains I and II) which was reported to contain the main 3CL^{pro} binding site [71]. Interestingly, in our predictions of the top-ranked poses, protonation of the ligand did not enhance its affinity for both protein targets (Tables **S2-S5**), suggesting that electrostatic interactions could not be determinant in the overall nucleopeptide-enzyme binding.

3.5. Evaluation of the Nucleopeptide as a Potential Anti-SARS-CoV-2 Drug

Due to the emerging role of machine learning (ML) and artificial intelligence (AI) as a potential aid for the understanding of nano-bio interactions in biomedical strategies, ML tools and ab initio simulations were recently adopted to improve the reproducibility of therapeutic data for robust quantitative comparisons and to facilitate in silico modelling and meta-analyses, leading to a substantial contribution to safe-by-design development in anti-viral/anti-microbial drug targets determination [72]. Physiologically based pharmacokinetic (PBPK) modelling and absorption, distribution, metabolism, and excretion (ADME)-based in silico methods along with drug dosimetry models are mainly employed in therapeutics/anti-infection compound development [73]. Conscious of the potential of in silico modelling in biomedicine, as well of the urgent need for anti-SARS-CoV-2 treatments [34, 74], we decided to conduct a more specific and detailed investigation of the anti-coronavirus potential of the nucleopeptide using the COVID-19 Docking Server [75], a web platform for docking small molecules, peptides or antibodies to COVID-19 protein targets. The main results of this study are reported in Table **2**. Interestingly, the nucleopeptide showed a high (or very high) affinity for the selected COVID-19 protein targets with binding energies ranging from -7.70 to -15.10 kcal/mol and RF scores varying between 6.50 and 7.93.

Table 2. COVID-19 Docking Server analysis of nucleopeptide anti-SARS-CoV-2 potential. Relevant protein targets, scoring function (RF-Score, pKd) and binding energy (score value, kcal/mol) values are reported.

Receptor from COVID-19 Docking Server	RF-Score (pKd)	Score value (Kcal/mol)
COVID-19 main protease (3CL^{pro})	6.51	-7.70
Papain-like protease	6.75	-11.50
Nsp3 (207-379, AMP site)	7.21	-10.80
Nsp3 (207-379, MES site)	6.69	-8.80
RdRp (RNA site, with RNA)	6.79	-12.00
RdRp (RNA site, without RNA)	6.93	-11.10
Helicase (ADP site)	6.83	-8.90
Helicase (NCB site)	6.67	-15.10
Nsp14 (ExoN)	6.68	-8.90
Nsp14 (N7-MTase)	6.76	-10.60
Nsp15 (endoribonuclease)	6.50	-8.90
Nsp16 (GTA site)	6.62	-8.00
Nsp16 (MGP site)	6.64	-9.00
Nsp16 (SAM site)	6.86	-7.90
N protein (NCB site)	7.93	-12.90

The binding energy predicted for the nucleopeptide-3CL^{pro} complex (-7.70 kcal/mol) was similar to the value (-8.06 kcal/mol) provided by SwissDock for the top-ranked pose (Table **S1**), and the structure of the complex (Fig. **S2**) largely resembled those shown in (Fig. **4**, bottom). Based on the predicted score values, the highest affinity was predicted for the Helicase (NCB site) of SARS-CoV-2, while other very high scores were found for N protein (NCB site), RdRp (RNA site), Papain-like protease and Nsp14 (N7-MTase). The tight nucleopeptide-RdRp binding predicted by the COVID-19 Docking Server particularly attracted our attention for the importance of RdRp inhibitors in the fight against SARS-CoV-2. In fact, the only FDA-approved drug for COVID-19 available to date, *i.e.* Remdesivir [76], is a RdRp binding substrate believed to inhibit this crucial SARS-CoV-2 enzyme.

An even higher score for RdRp was revealed when the polymerase was complexed with RNA, with respect to the same target lacking the ribonucleic acid. In the former case, the nucleopeptide binds in a slightly different manner the target being closer to the RNA present in the complex, as can be observed from the predictive structure analysis in Fig. (**S2**). To find an explanation for the more favourable energy score for the complex with RNA, we examined in more detail the complexes formed by the nucleopeptide with the viral RNA polymerase, as visualized in the structure viewer of the COVID-19 Docking Server (Fig. **5**).
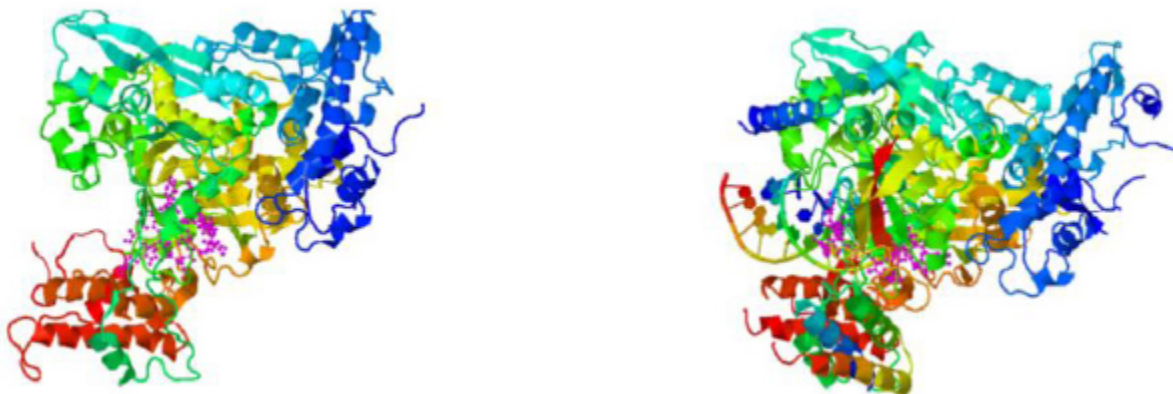
Fig. (5). Top ranked pose (**Top 1**) views of nucleopeptide-RdRp (**left**) and nucleopeptide-RdRp+RNA (**right**) complexes predicted by COVID-19 Docking Server. (*A higher resolution / colour version of this figure is available in the electronic copy of the article*).

We found that the nucleopeptide in complex with RdRp+RNA had more contacts compared to the complex with RdRp without RNA substrate, involving in the overall binding process the interaction of the nucleopeptide with the RNA molecule itself as shown by analyzing the top-ranked complex with UCSF Chimera that revealed multiple interactions between the ligand and the RNA (data not shown). On the other hand, according to the score values nucleopeptide binding affinity for the protein in the presence of RNA is higher not only in case of the top-ranked poses (Fig. **5**) but also considering the other poses ranging from 1-6 (Table **S6**).

CONCLUSION

Our studies provided new insights on a nucleopeptide based on L-diaminopropanoic acid. This molecule, whose morphology in the solid phase was studied by SEM, was able to adopt different conformations, passing from a more to a less stacked structure upon heating, as revealed by spectroscopy. Moreover, the protein binding ability of the nucleopeptide was demonstrated by CD, revealing for BSA a perturbation effect on the protein helical structure caused by the ligand. SwissDock docking studies indicated a predicted binding energy of about -12 kcal/mol for the complex BSA-nucleopeptide and showed interactions of the nucleopeptide with BSA helical regions in line with the CD data. A SwissDock docking of the nucleopeptide to the SARS-CoV-2 main protease 3CL^{pro} showed a good binding affinity and prompted us to investigate in more detail the potential for the nucleopeptide to target COVID-19 proteins. In this regard, a multiple docking experiment conducted with the COVID-19 Docking Server indicated the possible role of the nucleopeptide

as binder of several relevant COVID-19 protein targets and thus, as a potential drug active against SARS-CoV-2. High affinities were predicted for the nucleopeptide interaction with the coronavirus papain-like protease, with the helicase at the ribonucleotide-binding site and with the RNA-dependent RNA polymerase (RdRp). In the latter case, the complex nucleopeptide-RdRp was endowed with higher score values when the RNA substrate was embedded in the protein structure, suggesting the propensity of the nucleopeptide to interact with RNA structures even when in complex with proteins. Overall, this study furnishes novel descriptive elements of the nature of the nucleopeptide and provides precious information on the possibility to direct nucleobase-containing peptide drugs against protein targets, including those involved in current socially-relevant diseases.

LIST OF ABBREVIATIONS

ADME	=	Absorption, Distribution, Metabolism, and Excretion
ADP	=	Adenosine DiPhosphate
AI	=	Artificial Intelligence
AMP	=	Adenosine MonoPhosphate
BSA	=	Bovine Serum Albumin
CD	=	Circular Dichroism
3CL^{pro}	=	Chymotrypsin-like protease
COVID-19	=	COronaVIrus Disease 19
DNA	=	DeoxyriboNucleic Acid
ExoN	=	N-terminal ExoriboNuclease

GTA	=	P1-7-methylGuanosine-P3-Adenosine-5',5'-Triphosphate
HIV	=	Human Immunodeficiency Virus
MES	=	2-(N-Morpholino)-EthaneSulfonic acid
MGP	=	7-Methyl-Guanosine- 5'-triPhosphate
ML	=	Machine Learning
MMLV	=	Moloney Murine Leukemia Virus
NCB	=	riboNucleotide-Binding
N7-MTase	=	guanine-N7 methyl transferase
N protein	=	Nucleocapsid protein
NSP	=	NonStructural Protein
PBPK	=	Physiologically based pharmacokinetic
PBS	=	Phosphate Buffer Saline
PL^{pro}	=	Papain-Like Protease
RdRp	=	RNA-dependent RNA Polymerase
RNA	=	RiboNucleic Acid
RT	=	Reverse Transcriptase
RTP	=	Remdesivir Triphosphate
SAM	=	S-adenosylmethionine
SARS-CoV-2	=	Severe Acute Respiratory Syndrome Coronavirus 2
SEM	=	Scanning Electron Microscopy

ETHICS APPROVAL AND CONSENT TO PARTICIPATE

Not applicable.

HUMAN AND ANIMAL RIGHTS

No humans/animals were used in the study that is the basis of this research.

CONSENT FOR PUBLICATION

Not applicable.

FUNDING

CONFLICT OF INTEREST

The author declares no conflict of interest, financial or otherwise.

ACKNOWLEDGEMENTS

SUPPLEMENTARY MATERIAL

Supplementary material is available on the publisher's website along with the published material.

REFERENCES

[1] Roviello, G.N.; Vicidomini, C.; Di Gaetano, S.; Capasso, D.; Musumeci, D.; Roviello, V. Solid phase synthesis and RNA-binding activity of an arginine-containing nucleopeptide. *RSC Advances,* **2016**, *6*(17), 14140-14148.
http://dx.doi.org/10.1039/C5RA25809J PMID: 29057071

[2] Musumeci, D.; Mokhir, A.; Roviello, G.N. Synthesis and nucleic acid binding evaluation of a thyminyl l-diaminobutanoic acid-based nucleopeptide. *Bioorg. Chem.,* **2020**, *100*, 103862.
http://dx.doi.org/10.1016/j.bioorg.2020.103862 PMID: 32428744

[3] Geotti-Bianchini, P.; Beyrath, J.; Chaloin, O.; Formaggio, F.; Bianco, A. Design and synthesis of intrinsically cell-penetrating nucleopeptides. *Org. Biomol. Chem.,* **2008**, *6*(20), 3661-3663.

http://dx.doi.org/10.1039/b811639c PMID: 18843393

[4]   Roviello, G.N.; Benedetti, E.; Pedone, C.; Bucci, E.M. Nucleobase-containing peptides: an overview of their characteristic features and applications. *Amino Acids,* **2010**, *39*(1), 45-57.
http://dx.doi.org/10.1007/s00726-010-0567-6   PMID: 20349320

[5]   Roviello, G.; Musumeci, D.; Castiglione, M.; Bucci, E.M.; Pedone, C.; Benedetti, E. Solid phase synthesis and RNA-binding studies of a serum-resistant nucleo-epsilon-peptide. *J. Pept. Sci.,* **2009**, *15*(3), 155-160.
http://dx.doi.org/10.1002/psc.1072 PMID: 18985708

[6]   De Napoli, L.; Messere, A.; Montesarchio, D.; Piccialli, G.; Benedetti, E.; Bucci, E.; Rossi, F. A new solid-phase synthesis of oligonucleotides 3′-conjugated with peptides. *Bioorg. Med. Chem.,* **1999**, *7*(2), 395-400.
http://dx.doi.org/10.1016/S0968-0896(98)00250-8 PMID: 10218834

[7]   Roviello, G.N.; Roviello, G.; Musumeci, D.; Bucci, E.M.; Pedone, C. Dakin-West reaction on 1-thyminyl acetic acid for the synthesis of 1,3-bis(1-thyminyl)-2-propanone, a heteroaromatic compound with nucleopeptide-binding properties. *Amino Acids,* **2012**, *43*(4), 1615-1623.
http://dx.doi.org/10.1007/s00726-012-1237-7   PMID: 22349760

[8]   Oliviero, G.; Amato, J.; Borbone, N.; D’Errico, S.; Piccialli, G.; Bucci, E.; Piccialli, V.; Mayol, L. Synthesis of 4-N-alkyl and ribose-modified AICAR analogues on solid support. *Tetrahedron,* **2008**, *64*(27), 6475-6481.
http://dx.doi.org/10.1016/j.tet.2008.04.071

[9]   Oliviero, G.; Amato, J.; Borbone, N.; D’Errico, S.; Piccialli, G.; Mayol, L. Synthesis of N-1 and ribose modified inosine analogues on solid support. *Tetrahedron Lett.,* **2007**, *48*(3), 397-400.
http://dx.doi.org/10.1016/j.tetlet.2006.11.085

[10]   Oliviero, G.; D’Errico, S.; Borbone, N.; Amato, J.; Piccialli, V.; Varra, M.; Piccialli, G.; Mayol, L. A solid-phase approach to the synthesis of N-1-alkyl analogues of cyclic inosine-diphosphate-ribose (cIDPR). *Tetrahedron,* **2010**, *66*(10), 1931-1936.
http://dx.doi.org/10.1016/j.tet.2010.01.013

[11]   D’Errico, S.; Oliviero, G.; Amato, J.; Borbone, N.; Cerullo, V.; Hemminki, A.; Piccialli, V.; Zaccaria, S.; Mayol, L.; Piccialli, G. Synthesis and biological evaluation of unprecedented ring-expanded nucleosides (RENs) containing the imidazo[4,5-d][1,2,6]oxadiazepine ring system. *Chem. Commun. (Camb.),* **2012**, *48*(74), 9310-9312.
http://dx.doi.org/10.1039/c2cc33511e PMID: 22874871

[12]   Oliviero, G.; D’Errico, S.; Borbone, N.; Amato, J.; Piccialli, V.; Piccialli, G.; Mayol, L. Facile solid-phase synthesis of AICAR 5′-monophosphate (ZMP) and its 4-N-alkyl derivatives. *Eur. J. Org. Chem.,* **2010**, *2010*(8), 1517-1524.
http://dx.doi.org/10.1002/ejoc.200901271

[13]   D’Errico, S.; Oliviero, G.; Borbone, N.; Amato, J.; D’Alonzo, D.; Piccialli, V.; Mayol, L.; Piccialli, G. A facile synthesis of 5′-fluoro-5′-deoxyacadesine (5′-F-AICAR): a novel non-phosphorylable AICAR analogue. *Molecules,* **2012**, *17*(11), 13036-13044.
http://dx.doi.org/10.3390/molecules171113036   PMID: 23124472

[14]   Roviello, G.N. Novel insights into nucleoamino acids: biomolecular recognition and aggregation studies of a thymine-conjugated L-phenyl alanine. *Amino Acids,* **2018**, *50*(7), 933-941.
http://dx.doi.org/10.1007/s00726-018-2562-2   PMID: 29766280

[15]   Dolman, N.P.; More, J.C.A.; Alt, A.; Knauss, J.L.; Troop, H.M.; Bleakman, D.; Collingridge, G.L.; Jane, D.E. Structure-activity relationship studies on N3-substituted willardiine derivatives acting as AMPA or kainate receptor antagonists. *J. Med. Chem.,* **2006**, *49*(8), 2579-2592.
http://dx.doi.org/10.1021/jm051086f PMID: 16610801

[16]   Roviello, G.N.; Ricci, A.; Bucci, E.M.; Pedone, C. Synthesis, biological evaluation and supramolecular assembly of novel analogues of peptidyl nucleosides. *Mol. Biosyst.,* **2011**, *7*(5), 1773-1778.
http://dx.doi.org/10.1039/c1mb05007a PMID: 21431179

[17]   Walsh, C.T.; Zhang, W. Chemical logic and enzymatic machinery for biological assembly of peptidyl nucleoside antibiotics. *ACS Chem. Biol.,* **2011**, *6*(10), 1000-1007.
http://dx.doi.org/10.1021/cb200284p PMID: 21851099

[18]   De, S.; Groaz, E.; Margamuljana, L.; Herdewijn, P. Syntheses of 5′-nucleoside monophosphate derivatives with unique aminal, hemiaminal, and hemithioaminal functionalities: a new class of 5′-peptidyl nucleotides. *Chemistry,* **2016**, *22*(24), 8167-8180.
http://dx.doi.org/10.1002/chem.201600721   PMID: 27136602

[19]   Roviello, G.N.; Oliviero, G.; Di Napoli, A.; Borbone, N.; Piccialli, G. Synthesis, self-assembly-behavior and biomolecular recognition properties of thyminyl dipeptides. *Arab. J. Chem.,* **2020**, *13*(1), 1966-1974.
http://dx.doi.org/10.1016/j.arabjc.2018.02.014

[20]   Wang, H.; Feng, Z.; Qin, Y.; Wang, J.; Xu, B. Nucleopeptide assemblies selectively sequester ATP in cancer cells to increase the efficacy of doxorubicin. *Angew. Chem. Int. Ed. Engl.,* **2018**, *57*(18), 4931-4935.
http://dx.doi.org/10.1002/anie.201712834   PMID: 29451962

[21]   Wang, H.; Feng, Z.; Xu, B. Supramolecular assemblies of peptides or nucleopeptides for gene delivery. *Theranostics,* **2019**, *9*(11), 3213-3222.
http://dx.doi.org/10.7150/thno.31854 PMID: 31244950

[22]   Baek, K.; Noblett, A.D.; Ren, P.; Suggs, L.J. Self-assembled nucleo-tripeptide hydrogels provide local and sustained doxorubicin release. *Biomater. Sci.,* **2020**, *8*(11), 3130-3137.
http://dx.doi.org/10.1039/D0BM00134A PMID: 32352097

[23]   Watanabe, S.; Tomizaki, K.Y.; Takahashi, T.; Usui, K.; Kajikawa, K.; Mihara, H. Interactions between peptides containing nucleobase amino acids and T7 phages displaying *S. cerevisiae* proteins. *Biopolymers,* **2007**, *88*(2), 131-140.
http://dx.doi.org/10.1002/bip.20662 PMID: 17206624

[24]   Uozumi, R.; Takahashi, T.; Yamazaki, T.; Granholm, V.; Mihara, H. Design and conformational analysis of natively folded β-hairpin peptides stabilized by nucleobase interactions. *Biopolymers,* **2010**, *94*(6), 830-842.
http://dx.doi.org/10.1002/bip.21464 PMID: 20535820

[25]   Roviello, G.N.; Di Gaetano, S.; Capasso, D.; Franco, S.; Crescenzo, C.; Bucci, E.M.; Pedone, C. RNA-binding and viral reverse transcriptase inhibitory activity of a novel cationic diamino acid-based peptide. *J. Med. Chem.,* **2011**, *54*(7), 2095-2101.
http://dx.doi.org/10.1021/jm1012769 PMID: 21391685

[26]   Roviello, G.N.; Di Gaetano, S.; Capasso, D.; Cesarani, A.; Bucci, E.M.; Pedone, C. Synthesis, spectroscopic studies and biological activity of a novel nucleopeptide with Moloney murine leukemia virus reverse transcriptase inhibitory activity. *Amino Acids,* **2010**, *38*(5), 1489-1496.
http://dx.doi.org/10.1007/s00726-009-0361-5   PMID:

19813074

[27] Musumeci, D.; Roviello, V.; Roviello, G.N. DNA- and RNA-binding ability of oligoDapT, a nucleobase-decorated peptide, for biomedical applications. *Int. J. Nanomedicine,* **2018**, *13*, 2613-2629.
http://dx.doi.org/10.2147/IJN.S156381 PMID: 29750033

[28] Kelly, S.M.; Price, N.C. The use of circular dichroism in the investigation of protein structure and function. *Curr. Protein Pept. Sci.,* **2000**, *1*(4), 349-384.
http://dx.doi.org/10.2174/1389203003381315 PMID: 12369905

[29] Singh, A.V.; Jahnke, T.; Wang, S.; Xiao, Y.; Alapan, Y.; Kharratian, S.; Onbasli, M.C.; Kozielski, K.; David, H.; Richter, G. Anisotropic gold nanostructures: optimization *viain silico* modeling for hyperthermia. *ACS Appl. Nano Mater.,* **2018**, *1*(11), 6205-6216.
http://dx.doi.org/10.1021/acsanm.8b01406

[30] Singh, A.V.; Jahnke, T.; Xiao, Y.; Wang, S.; Yu, Y.; David, H.; Richter, G.; Laux, P.; Luch, A.; Srivastava, A.; Saxena, P.S.; Bill, J.; Sitti, M. Peptide-induced biomineralization of tin oxide (SnO$_2$) nanoparticles for antibacterial applications. *J. Nanosci. Nanotechnol.,* **2019**, *19*(9), 5674-5686.
http://dx.doi.org/10.1166/jnn.2019.16645 PMID: 30961724

[31] Singh, A.V.; Alapan, Y.; Jahnke, T.; Laux, P.; Luch, A.; Aghakhani, A.; Kharratian, S.; Onbasli, M.C.; Bill, J.; Sitti, M. Seed-mediated synthesis of plasmonic gold nanoribbons using cancer cells for hyperthermia applications. *J. Mater. Chem. B Mater. Biol. Med.,* **2018**, *6*(46), 7573-7581.
http://dx.doi.org/10.1039/C8TB02239A PMID: 32254879

[32] Tu, Y-F.; Chien, C-S.; Yarmishyn, A.A.; Lin, Y-Y.; Luo, Y-H.; Lin, Y-T.; Lai, W-Y.; Yang, D-M.; Chou, S-J.; Yang, Y-P.; Wang, M-L.; Chiou, S-H. A review of SARS-CoV-2 and the ongoing clinical trials. *Int. J. Mol. Sci.,* **2020**, *21*(7), 2657.
http://dx.doi.org/10.3390/ijms21072657 PMID: 32290293

[33] Wang, L.; Wang, Y.; Ye, D.; Liu, Q. Review of the 2019 novel coronavirus (SARS-CoV-2) based on current evidence. *Int. J. Antimicrob. Agents,* **2020**, *55*(6), 105948.
http://dx.doi.org/10.1016/j.ijantimicag.2020.105948 PMID: 32201353

[34] Costanzo, M.; De Giglio, M.A.R.; Roviello, G.N. SARS-CoV-2: recent reports on antiviral therapies based on lopinavir/ritonavir, darunavir/umifenovir, hydroxychloroquine, remdesivir, favipiravir and other drugs for the treatment of the new coronavirus. *Curr. Med. Chem.,* **2020**, *27*(27), 4536-4541.
http://dx.doi.org/10.2174/0929867327666200416131117 PMID: 32297571

[35] Freitas, B.T.; Durie, I.A.; Murray, J.; Longo, J.E.; Miller, H.C.; Crich, D.; Hogan, R.J.; Tripp, R.A.; Pegan, S.D. Characterization and noncovalent inhibition of the deubiquitinase and deisgylase activity of SARS-CoV-2 papain-like protease. *ACS Infect. Dis.,* **2020**, *6*(8), 2099-2109.
http://dx.doi.org/10.1021/acsinfecdis.0c00168 PMID: 32428392

[36] Roviello, V.; Roviello, G.N. Lower COVID-19 mortality in Italian forested areas suggests immunoprotection by Mediterranean plants. *Environ. Chem. Lett.,* **2020**, 1-12.
http://dx.doi.org/10.1007/s10311-020-01063-0 PMID: 32837486

[37] Habtemariam, S.; Nabavi, S.F.; Banach, M.; Berindan-Neagoe, I.; Sarkar, K.; Sil, P.C.; Nabavi, S.M. Should we try SARS-CoV-2 helicase inhibitors for COVID-19 therapy? *Arch. Med. Res.,* **2020**, *51*(7), 733-735.
http://dx.doi.org/10.1016/j.arcmed.2020.05.024 PMID: 32536457

[38] Zhu, W.; Chen, C.Z.; Gorshkov, K.; Xu, M.; Lo, D.C.; Zheng, W. RNA-dependent RNA polymerase as a target for COVID-19 drug discovery. *SLAS Discov.,* **2020**, *25*(10), 1141-1151.
http://dx.doi.org/10.1177/2472555220942123 PMID: 32660307

[39] Viparelli, F.; Cassese, A.; Doti, N.; Paturzo, F.; Marasco, D.; Dathan, N.A.; Monti, S.M.; Basile, G.; Ungaro, P.; Sabatella, M.; Miele, C.; Teperino, R.; Consiglio, E.; Pedone, C.; Beguinot, F.; Formisano, P.; Ruvo, M. Targeting of PED/PEA-15 molecular interaction with phospholipase D1 enhances insulin sensitivity in skeletal muscle cells. *J. Biol. Chem.,* **2008**, *283*(31), 21769-21778.
http://dx.doi.org/10.1074/jbc.M803771200 PMID: 18541525

[40] Roviello, G.N.; Moccia, M.; Sapio, R.; Valente, M.; Bucci, E.M.; Castiglione, M.; Pedone, C.; Perretta, G.; Benedetti, E.; Musumeci, D. Synthesis, characterization and hybridization studies of new nucleo-gamma-peptides based on diaminobutyric acid. *J. Pept. Sci.,* **2006**, *12*(12), 829-835.
http://dx.doi.org/10.1002/psc.819 PMID: 17131297

[41] Moccia, M.; Roviello, G.N.; Bucci, E.M.; Pedone, C.; Saviano, M. Synthesis of a l-lysine-based alternate alpha,epsilon-peptide: a novel linear polycation with nucleic acids-binding ability. *Int. J. Pharm.,* **2010**, *397*(1-2), 179-183.
http://dx.doi.org/10.1016/j.ijpharm.2010.06.044 PMID: 20599488

[42] Roviello, G.N.; Roviello, V.; Autiero, I.; Saviano, M. Solid phase synthesis of TyrT, a thymine-tyrosine conjugate with poly(A) RNA-binding ability. *RSC Advances,* **2016**, *6*(33), 27607-27613.
http://dx.doi.org/10.1039/C6RA00294C PMID: 29057072

[43] Roviello, G.N.; Crescenzo, C.; Capasso, D.; Di Gaetano, S.; Franco, S.; Bucci, E.M.; Pedone, C. Synthesis of a novel Fmoc-protected nucleoaminoacid for the solid phase assembly of 4-piperidyl glycine/L-arginine-containing nucleopeptides and preliminary RNA: interaction studies. *Amino Acids,* **2010**, *39*(3), 795-800.
http://dx.doi.org/10.1007/s00726-010-0532-4 PMID: 20204432

[44] Fik-Jaskółka, M.A.; Mkrtchyan, A.F.; Saghyan, A.S.; Palumbo, R.; Belter, A.; Hayriyan, L.A.; Simonyan, H.; Roviello, V.; Roviello, G.N. Spectroscopic and SEM evidences for G4-DNA binding by a synthetic alkyne-containing amino acid with anticancer activity. *Spectrochim. Acta A Mol. Biomol. Spectrosc.,* **2020**, *229*, 117884.
http://dx.doi.org/10.1016/j.saa.2019.117884 PMID: 31927477

[45] Oliviero, G.; Borbone, N.; Amato, J.; D'Errico, S.; Galeone, A.; Piccialli, G.; Varra, M.; Mayol, L. Synthesis of quadruplex-forming tetra-end-linked oligonucleotides: effects of the linker size on quadruplex topology and stability. *Biopolymers,* **2009**, *91*(6), 466-477.
http://dx.doi.org/10.1002/bip.21153 PMID: 19189376

[46] Di Natale, C.; Scognamiglio, P.L.; Cascella, R.; Cecchi, C.; Russo, A.; Leone, M.; Penco, A.; Relini, A.; Federici, L.; Di Matteo, A.; Chiti, F.; Vitagliano, L.; Marasco, D. Nucleophosmin contains amyloidogenic regions that are able to form toxic aggregates under physiological condi-

tions. *FASEB J.,* **2015**, *29*(9), 3689-3701.
http://dx.doi.org/10.1096/fj.14-269522 PMID: 25977257

[47] Saghyan, A.S.; Simonyan, H.M.; Petrosyan, S.G.; Ge-olchanyan, A.V.; Roviello, G.N.; Musumeci, D.; Roviello, V. Thiophenyl-substituted triazolyl-thione L-alanine: asymmetric synthesis, aggregation and biological properties. *Amino Acids,* **2014**, *46*(10), 2325-2332.
http://dx.doi.org/10.1007/s00726-014-1782-3 PMID: 24952728

[48] Marasco, D.; Vicidomini, C.; Krupa, P.; Cioffi, F.; Quoc Huy, P.D.; Suan Li, M.; Florio, D.; Broersen, K.; De Pandis, M.F.; Roviello, G.N. Plant isoquinoline alkaloids as potential neurodrugs: a comparative study of the effects of benzo[c]phenanthridine and berberine based compounds on β-amyloid aggregation. *Chem. Biol. Interact.,* **2020**, *109300*
http://dx.doi.org/10.1016/j.cbi.2020.109300 PMID: 33098838

[49] Roviello, G.N.; Musumeci, D.; Roviello, V. Cationic peptides as RNA compaction agents: a study on the polyA compaction activity of a linear alpha,epsilon-oligo-L-lysine. *Int. J. Pharm.,* **2015**, *485*(1-2), 244-248.
http://dx.doi.org/10.1016/j.ijpharm.2015.03.011 PMID: 25772417

[50] Micsonai, A.; Wien, F.; Bulyáki, É.; Kun, J.; Moussong, É.; Lee, Y-H.; Goto, Y.; Réfrégiers, M.; Kardos, J. BeStSel: a web server for accurate protein secondary structure prediction and fold recognition from the circular dichroism spectra. *Nucleic Acids Res.,* **2018**, *46*(W1), W315-W322.
http://dx.doi.org/10.1093/nar/gky497 PMID: 29893907

[51] Perez-Iratxeta, C.; Andrade-Navarro, M.A. K2D2: estimation of protein secondary structure from circular dichroism spectra. *BMC Struct. Biol.,* **2008**, *8*(1), 25.
http://dx.doi.org/10.1186/1472-6807-8-25 PMID: 18477405

[52] Musumeci, D.; Roviello, G.N.; Rigione, G.; Capasso, D.; Di Gaetano, S.; Riccardi, C.; Roviello, V.; Montesarchio, D. Benzodifuran derivatives as potential antiproliferative agents: possible correlation between their bioactivity and aggregation properties. *ChemPlusChem,* **2017**, *82*(2), 251-260.
http://dx.doi.org/10.1002/cplu.201600547 PMID: 31961558

[53] Diaferia, C.; Sibillano, T.; Giannini, C.; Roviello, V.; Vitagliano, L.; Morelli, G.; Accardo, A. Photoluminescent peptide-based nanostructures as fret donor for fluorophore dye. *Chemistry,* **2017**, *23*(36), 8741-8748.
http://dx.doi.org/10.1002/chem.201701381 PMID: 28508550

[54] Gattuso, C.; Campanella, L.; Giosafatto, C.V.L.; Mariniello, L.; Roviello, V. The consolidating and adhesive properties of funori: microscopy findings on common and ancient paper samples. *J. Cult. Herit.,* **2021**, *48*, 153-160.
http://dx.doi.org/10.1016/j.culher.2020.11.013

[55] Burley, S.K.; Berman, H.M.; Bhikadiya, C.; Bi, C.; Chen, L.; Costanzo, L.D.; Christie, C.; Duarte, J.M.; Dutta, S.; Feng, Z.; Ghosh, S.; Goodsell, D.S.; Green, R.K.; Guranovic, V.; Guzenko, D.; Hudson, B.P.; Liang, Y.; Lowe, R.; Peisach, E.; Periskova, I.; Randle, C.; Rose, A.; Sekharan, M.; Shao, C.; Tao, Y-P.; Valasatava, Y.; Voigt, M.; Westbrook, J.; Young, J.; Zardecki, C.; Zhuravleva, M.; Kurisu, G.; Nakamura, H.; Kengaku, Y.; Cho, H.; Sato, J.; Kim, J.Y.; Ikegawa, Y.; Nakagawa, A.; Yamashita, R.; Kudou, T.; Bekker, G-J.; Suzuki, H.; Iwata, T.; Yokochi, M.; Kobayashi, N.; Fujiwara, T.; Velankar, S.;

Kleywegt, G.J.; Anyango, S.; Armstrong, D.R.; Berrisford, J.M.; Conroy, M.J.; Dana, J.M.; Deshpande, M.; Gane, P.; Gáborová, R.; Gupta, D.; Gutmanas, A.; Koča, J.; Mak, L.; Mir, S.; Mukhopadhyay, A.; Nadzirin, N.; Nair, S.; Patwardhan, A.; Paysan-Lafosse, T.; Pravda, L.; Salih, O.; Sehnal, D.; Varadi, M.; Vařeková, R.; Markley, J.L.; Hoch, J.C.; Romero, P.R.; Baskaran, K.; Maziuk, D.; Ulrich, E.L.; Wedell, J.R.; Yao, H.; Livny, M.; Ioannidis, Y.E. Protein data bank: the single global archive for 3D macromolecular structure data. *Nucleic Acids Res.,* **2019**, *47*(D1), D520-D528.
http://dx.doi.org/10.1093/nar/gky949 PMID: 30357364

[56] Grosdidier, A.; Zoete, V.; Michielin, O. SwissDock, a protein-small molecule docking web service based on EADock DSS. *Nucleic Acids Res,* **2011**, *39*(Web Server issue)(Suppl.), W270-W277.
http://dx.doi.org/10.1093/nar/gkr366

[57] Haberthür, U.; Caflisch, A. FACTS: Fast analytical continuum treatment of solvation. *J. Comput. Chem.,* **2008**, *29*(5), 701-715.
http://dx.doi.org/10.1002/jcc.20832 PMID: 17918282

[58] Pettersen, E.F.; Goddard, T.D.; Huang, C.C.; Couch, G.S.; Greenblatt, D.M.; Meng, E.C.; Ferrin, T.E. UCSF Chimera-a visualization system for exploratory research and analysis. *J. Comput. Chem.,* **2004**, *25*(13), 1605-1612.
http://dx.doi.org/10.1002/jcc.20084 PMID: 15264254

[59] Kong, R.; Wang, F.; Zhang, J.; Wang, F.; Chang, S. codockpp: a multistage approach for global and site-specific protein-protein docking. *J. Chem. Inf. Model.,* **2019**, *59*(8), 3556-3564.
http://dx.doi.org/10.1021/acs.jcim.9b00445 PMID: 31276391

[60] Trott, O.; Olson, A.J. AutoDock vina: improving the speed and accuracy of docking with a new scoring function, efficient optimization, and multithreading. *J. Comput. Chem.,* **2010**, *31*(2), 455-461.
http://dx.doi.org/10.1002/jcc.21334 PMID: 19499576

[61] Li, H.; Leung, K-S.; Wong, M-H.; Ballester, P.J. Correcting the impact of docking pose generation error on binding affinity prediction. *BMC Bioinformatics,* **2016**, *17*(S11)(Suppl. 11), 308.
http://dx.doi.org/10.1186/s12859-016-1169-4 PMID: 28185549

[62] Kong, R.; Yang, G.; Xue, R.; Liu, M.; Wang, F.; Hu, J.; Guo, X.; Chang, S.; Ponty, Y. COVID-19 docking server: a meta server for docking small molecules, peptides and antibodies against potential targets of COVID-19. *Bioinformatics,* **2020**, *36*(20), 5109-5111.
http://dx.doi.org/10.1093/bioinformatics/btaa645 PMID: 32692801

[63] Trott, O.; Olson, A.J. AutoDock vina: improving the speed and accuracy of docking with a new scoring function, efficient optimization, and multithreading. *J. Comput. Chem.,* **2010**, *31*(2), 455-461.
http://dx.doi.org/10.1002/jcc.21334 PMID: 19499576

[64] Zhang, S.; Holmes, T.C.; DiPersio, C.M.; Hynes, R.O.; Su, X.; Rich, A. Self-complementary oligopeptide matrices support mammalian cell attachment. *Biomaterials,* **1995**, *16*(18), 1385-1393.
http://dx.doi.org/10.1016/0142-9612(95)96874-Y PMID: 8590765

[65] Chinnathambi, S.; Karthikeyan, S.; Velmurugan, D.; Hanagata, N.; Aruna, P.; Ganesan, S. Effect of moderate UVC irradiation on bovine serum albumin and complex with antimetabolite 5-fluorouracil: fluorescence spectroscopic and

molecular modelling studies. *Int. J. Spectrosc.,* **2015**, *2015*, 315764.
http://dx.doi.org/10.1155/2015/315764

[66] Bujacz, A. Structures of bovine, equine and leporine serum albumin. *Acta Crystallogr. D Biol. Crystallogr.,* **2012**, *68*(Pt 10), 1278-1289.
http://dx.doi.org/10.1107/S0907444912027047 PMID: 22993082

[67] Owen, C.; Lukacik, P.; Strain-Damerell, C.; Douangamath, A.; Powell, A.; Fearon, D.; Brandao-Neto, J.; Crawshaw, A.; Aragao, D.; Williams, M 6Y84: SARS-CoV-2 main protease with unliganded active site (2019-nCoV, coronavirus disease 2019, COVID-19).*RCSB Protein Data Bank,* **2020**.

[68] Grosdidier, A.; Zoete, V.; Michielin, O. SwissDock, a protein-small molecule docking web service based on EADock DSS. *Nucleic Acids Res.,* **2011**, *39*(Web Server issue)(-Suppl. 2), W270-7.
http://dx.doi.org/10.1093/nar/gkr366 PMID: 21624888

[69] De Azevedo, W.F. Jr. *Docking screens for drug discovery*; Springer, **2019**, 2053, pp. 189-202.
http://dx.doi.org/10.1007/978-1-4939-9752-7_12

[70] Kumar, N.; Awasthi, A.; Kumari, A.; Sood, D.; Jain, P.; Singh, T.; Sharma, N.; Grover, A.; Chandra, R. Antitussive noscapine and antiviral drug conjugates as arsenal against COVID-19: a comprehensive chemoinformatics analysis. *J. Biomol. Struct. Dyn.,* **2020**> , 1-16.
http://dx.doi.org/10.1080/07391102.2020.1808072 PMID: 32815796

[71] Tahir ul Qamar, M; Alqahtani, S.M.; Alamri, M.A.; Chen, L.-L. Structural basis of SARS-CoV-2 3CLpro and anti--COVID-19 drug discovery from medicinal plants. *J. Pharm. Anal,* **2020**, *10*(4), 313-319.
http://dx.doi.org/10.1016/j.jpha.2020.03.009

[72] Singh, A.V.; Rosenkranz, D.; Ansari, M.H.D.; Singh, R.; Kanase, A.; Singh, S.P.; Johnston, B.; Tentschert, J.; Laux, P.; Luch, A. Artificial intelligence and machine learning empower advanced biomedical material design to toxicity prediction. *Advanced Intelligent Systems,* **2020**, *2*(12), 2000084.
http://dx.doi.org/10.1002/aisy.202000084

[73] Singh, A.V.; Ansari, M.H.D.; Rosenkranz, D.; Maharjan, R.S.; Kriegel, F.L.; Gandhi, K.; Kanase, A.; Singh, R.; Laux, P.; Luch, A. Artificial intelligence and machine learning in computational nanotoxicology: unlocking and empowering nanomedicine. *Adv. Healthc. Mater.,* **2020**, *9*(17), e1901862.
http://dx.doi.org/10.1002/adhm.201901862 PMID: 32627972

[74] Tiwari Pandey, A.; Pandey, I.; Zamboni, P.; Gemmati, D.; Kanase, A.; Singh, A.V.; Singh, M.P. Traditional herbal remedies with a multifunctional therapeutic approach as an implication in covid-19 associated co-infections. *Coatings,* **2020**, *10*(8), 761.
http://dx.doi.org/10.3390/coatings10080761

[75] Kong, R.; Yang, G.; Xue, R.; Liu, M.; Wang, F.; Hu, J.; Guo, X.; Chang, S. COVID-19 Docking Server: a meta server for docking small molecules, peptides and antibodies against potential targets of COVID-19. *Bioinformatics,* **2020**, *36*(20), 5109-5111.
http://dx.doi.org/10.1093/bioinformatics/btaa645 PMID: 32692801

[76] Twomey, J.D.; Luo, S.; Dean, A.Q.; Bozza, W.P.; Nalli, A.; Zhang, B. COVID-19 update: The race to therapeutic development. *Drug Resist. Updat.,* **2020**, *53*, 100733.
http://dx.doi.org/10.1016/j.drup.2020.100733 PMID: 33161277